J. CHEM. SOC. FARADAY TRANS., 1994, 90(21), 3357–3365

Oxidative Coupling of Methane over La_2O_3

Influence of Catalyst Preparation on Surface Properties and Steady and Oscillating Reaction Behaviour

V. R. Choudhary* and V. H. Rane
Chemical Engineering Division, National Chemical Laboratory, Pune 411 008, India

The catalyst precursor and calcination conditions used in the preparation of La_2O_3 have been found to have a marked influence on the surface properties, basicity and base strength distribution, and catalytic activity and selectivity in the oxidative coupling of methane (OCM) under different reaction conditions. Among the La_2O_3 catalysts, only that prepared from lanthanum acetate by decomposition in N_2 (but not in O_2) showed symmetric temperature and concentration oscillations in OCM at or below 933 K over a narrow temperature range. The unsteady reaction behaviour is found to be very complex and strongly dependent upon the OCM process parameters and the catalyst parameters. Furthermore, the results on the La_2O_3 obtained from the acetate indicated a strong possibility of the formation of new catalytic sites active at lower temperatures (below 873 K) during the OCM reaction at higher temperatures.

Earlier studies[1–7] showed that La_2O_3 has high activity and selectivity in OCM to C_2 hydrocarbons. La_2O_3 catalysts with promoters such as Li,[8] LiCl,[9] Na,[10], Sr[11–17] and Ba[18] have been studied as well as La-promoted MgO and CaO.[19–22] Taylor and Schrader[6] reported that La_2O_3 obtained from different precursors showed different catalytic performance in the OCM process. Recently we have observed unsteady reaction behaviour, with periodic fluctuations in reaction temperature and concentration indicating symmetric oscillations, in OCM (above 823 K but below 973 K) over La_2O_3 obtained from lanthanum acetate by thermal decomposition in N_2.[23] We have now investigated the influence of precursor and reaction conditions on the bulk and surface properties of La_2O_3 and also on the catalytic activity and selectivity and unsteady reaction behaviour in OCM under different process conditions.

Experimental

The La_2O_3 catalysts (Table 1) were prepared by thermal decomposition of different precursors. The hydrated La_2O_3 was prepared by treating powdered La_2O_3 (Aldrich) with deionized water (2 ml g^{-1}) on a water bath for 4 h while maintaining a constant water content of the slurry, followed by drying at 393 K for 12 h. The lanthanum acetate (Aldrich) and lanthanum nitrate (GR, Loba) were ground with deionized water sufficient to form a thick paste and dried at 393 K for 12 h. The lanthanum hydroxide, lanthanum carbonate (I and II) were prepared by precipitation from an aqueous solution of ammonium hydroxide, sodium carbonate or ammonium carbonate, respectively, at pH 10–11 at room temperature. The precipitate was washed with deionized water until free from cations and anions, and dried at 393 K for 12 h. The dried catalyst mass was decomposed at 873 K for 6 h in static air, pressed binder-free and crushed to 22–30 mesh size particles, then calcined at 1023 and 1223 K in a flow of N_2 or O_2 (12 000 cm^3 g^{-1} h^{-1}). The calcination conditions of the catalysts are given in Table 1.

The surface area of the catalysts calcined at 1023 and 1223 K was determined by the single-point BET method by measuring the adsorption of nitrogen (30 mol% in He) at liquid-nitrogen temperature, using a Monosorb surface-area analyser (Quanta Chrome Corp.). The crystal size and morphology of the catalysts were studied by scanning electron microscopy (SEM). The crystal phases were studied by powder X-ray diffraction (XRD).

The acidity distribution on the catalysts was determined by temperature-programmed desorption (TPD) of ammonia

Table 1 Catalyst precursors and calcination conditions

catalyst	precursor	calcination conditions[a] T/K	calcination conditions[a] atmosphere[b]	surface area /m^2 g^{-1}
I*a*	hydrated La_2O_3	1223	N_2	3.8
I*b*	hydrated La_2O_3	1023	N_2	6.3
II*a*	lanthanum acetate	1223	N_2	2.8
II*b*	lanthanum acetate	1023	N_2	4.5
II*c*	lanthanum acetate	1023	O_2	4.4
III*a*	lanthanum nitrate	1223	N_2	1.7
III*b*	lanthanum nitrate	1023	N_2	4.4
IV*a*	lanthanum carbonate (I)	1223	N_2	0.4
IV*b*	lanthanum carbonate (I)	1023	N_2	3.0
V*a*	lanthanum carbonate (II)	1223	N_2	2.0
V*b*	lanthanum carbonate (II)	1023	N_2	2.1
VI*a*	lanthanum hydroxide	1223	N_2	2.7
VI*b*	lanthanum hydroxide	1023	N_2	22.1

[a] Before calcination, catalyst precursor was decomposed at 873 K in static air for 6 h. The period of catalyst calcination was 2 h.
[b] Space velocity, 12 000 cm^3 g^{-1} h^{-1}.

(chemisorbed at 323 K) on the catalyst (0.5 g) from 323 to 1223 K at a linear heating rate of 20 °C min^{-1} in a flow of moisture-free helium (20 cm^3 min^{-1}) in a quartz reactor. The desorbed ammonia was detected with a thermal conductivity detector and also measured quantitatively by chemical analysis.[7]

The basicity and base-strength distribution on the catalysts were determined by measuring the step-wise thermal desorption (STD) of CO_2 from the catalyst (0.5 g) in a quartz reactor, from 323 to 1173 K in a number of successive temperature steps (*i.e.* 323–423, 423–573, 573–773, 773–973 and 973–1173 K). After the maximum temperature of the respective step was attained, it was maintained for a period of 30 min to allow desorption of the CO_2 adsorbed reversibly on the catalyst at that temperature. The amount of CO_2 desorbed in each step was determined gravimetrically by absorption in an aqueous barium hydroxide solution. The detailed procedure for measuring the base-strength distribution by the STD of CO_2 and the estimation of CO_2 chemisorption data from the STD data have been described earlier.[7,24] The CO_2 chemisorption data reported here are presented after subtracting the CO_2 content of the catalyst, which was determined by measuring the CO_2 evolved when the catalyst (after pretreatment at the calcination temperature in an He flow for 1 h) was heated from its calcination temperature to 1273 K in a flow of pure He for 1 h. Throughout, the chemisorption is considered as the amount of adsorbate retained by the presaturated catalyst after it was swept with pure He or N_2 for a period of 30 min.

The steady/unsteady OCM reaction over the catalysts was carried out in a tubular quartz flow reactor packed with catalyst particles (0.1–0.2 g) between quartz wool plugs. The reactor was kept in a vertical tubular furnace. The reaction temperature (controlled by a digital proportional temperature controller) was measured by a chromel–alumel thermocouple located in the catalyst bed. The temperature under unsteady conditions was measured as a function of reaction time. The reaction was carried out under following conditions: amount of catalyst, 0.1–0.2 g; feed, pure CH_4–O_2; CH_4/O_2, 3.0–8.0; space velocity, 51 600–103 200 cm^3 g^{-1} h^{-1} and temperature, *i.e.* reactor temperature, 673–1123 K.

The product gases after the removal of water by condensation at 273 K were analysed by an on-line gas chromatograph using Porapak-Q and Spherocarb columns. The concentration of O_2 in the product stream was recorded continuously by an on-line paramagnetic O_2-analyser (Oxymat I, Fuji Electric).

High-purity gases He (>99.99%), CH_4 (99.995%), CO_2 (99.995%), O_2 (>99.5%) and NH_3 (99.99%) were used.

Before being used the catalysts were pretreated *in situ* at their calcination temperature in a flow of He (20 cm^3 min^{-1}) for 1 h.

Results and Discussion

Surface Properties

The surface areas of the catalysts are included in Table 1. The surface area of La_2O_3 is strongly influenced by the precursors and the calcination temperature.

The SEM micrographs of La_2O_3 (I*b*–VI*b*) are presented in Fig. 1 and that of La_2O_3 (II*a*) and La_2O_3 (II*c*) in Fig. 2. A comparison of the SEM photographs of La_2O_3 (I*b*–VI*b*)

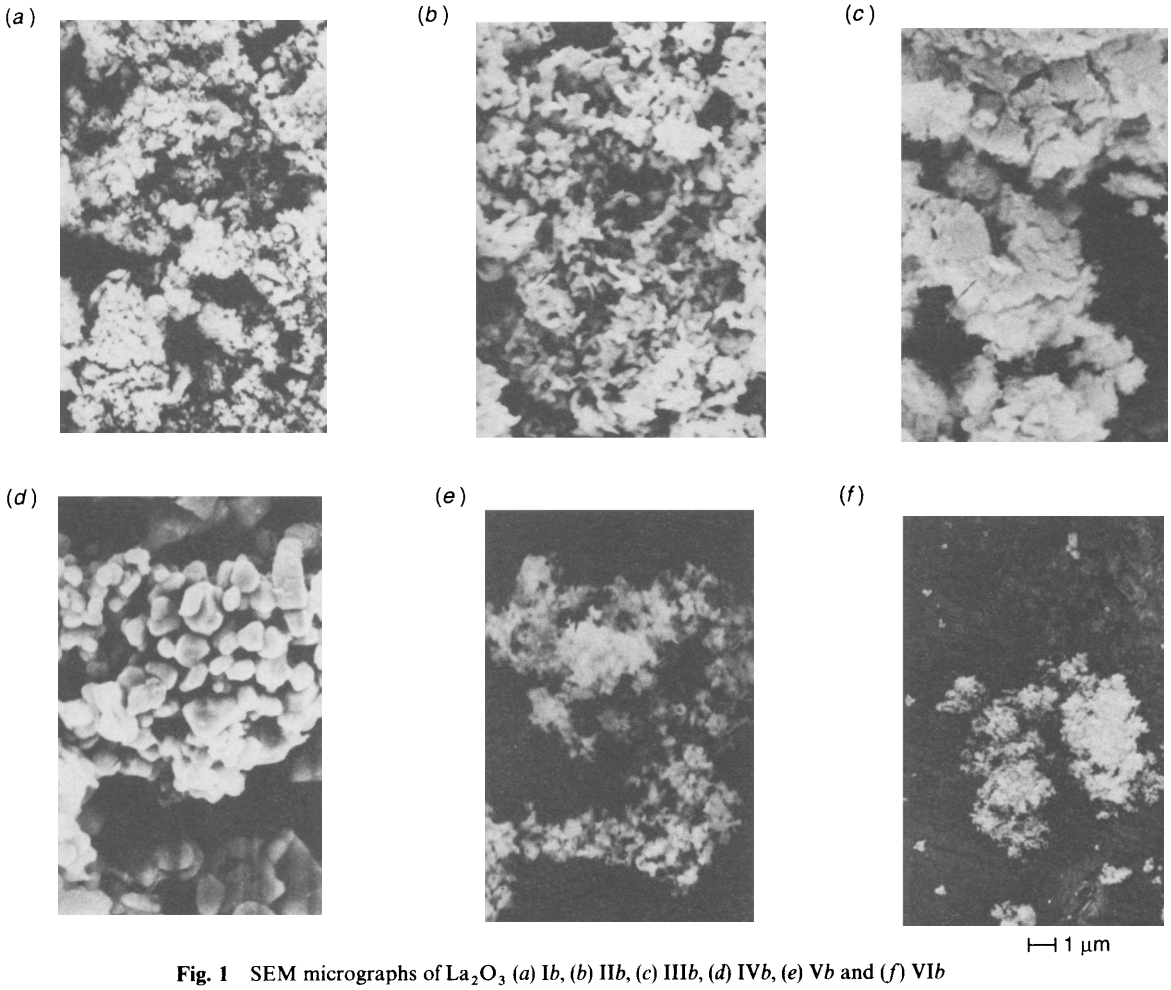

Fig. 1 SEM micrographs of La_2O_3 (*a*) I*b*, (*b*) II*b*, (*c*) III*b*, (*d*) IV*b*, (*e*) V*b* and (*f*) VI*b*

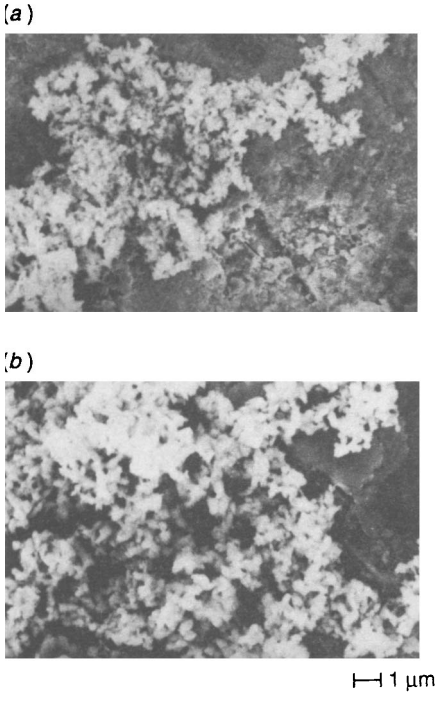

Fig. 2 SEM micrographs of La_2O_3 obtained by calcination of La acetate (*a*) at 1023 K in O_2 flow for 2 h and (*b*) at 1223 K in N_2 flow for 2 h

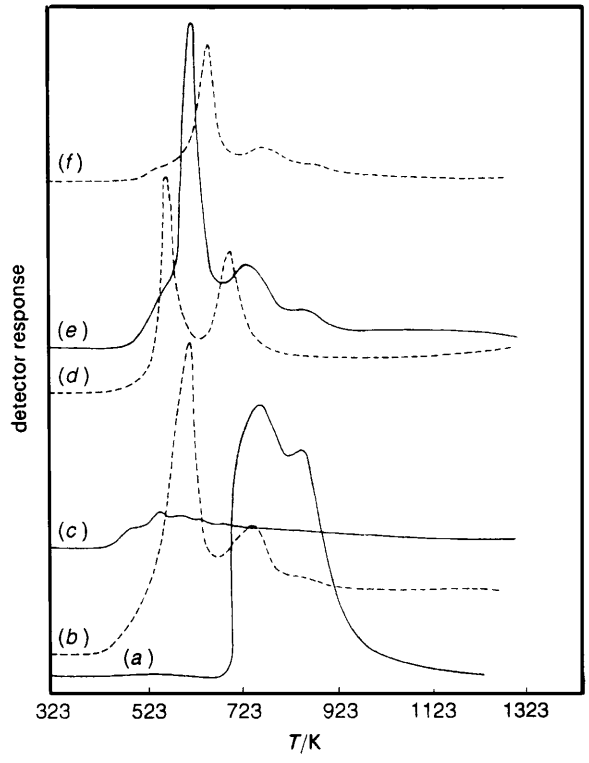

Fig. 3 TPD of ammonia on (*a*) I*a*, θ_i = 1.69 mmol g^{-1}; (*b*) II*a*, θ_i = 0.69 mmol g^{-1}; (*c*) III*a*, θ_i = 0.24 mmol g^{-1}; (*d*) IV*a*, θ_i = 0.23 mmol g^{-1}; (*e*) V*a*, θ_i = 0.18 mmol g^{-1}; (*f*) VI*a*, θ_i = 0.17 mmol g^{-1}

shows a strong influence of the precursor on the crystal size and morphology. Furthermore, a comparison of the SEM micrographs of La_2O_3 (II*a*, II*b* and II*c*) indicates that the crystal size and morphology of La_2O_3 (II) is influenced by the temperature and gas atmosphere used in the catalyst calcination.

XRD analysis of the La_2O_3 (I–VI*a*) catalysts obtained by the decomposition and calcination of the different catalyst precursors at 1223 K has indicated the presence of only pure La_2O_3 crystalline phase. The La_2O_3 (I*b*, III*b* and VI*b*) catalysts were also found to contain only the La_2O_3 phase but the La_2O_3 (II*b*, IV*b* and V*b*) obtained from lanthanum acetate and lanthanum carbonate also showed the presence of minor amounts of $La_2(CO_3)_3$ and $La_2O_2CO_3$ (lanthanum oxycarbonate). The XRD data have been presented elsewhere.[25]

The XRD results indicate no lanthanum carbonate or oxycarbonate to be present in the catalysts calcined at 1223 K. However, these carbonates are not completely decomposed at 1023 K and hence are retained to a small extent in the bulk of the catalysts obtained from the decomposition of lanthanum acetate or carbonates. These observations are quite consistent with earlier studies.[6,26,27]

The CO_2 content of II*b*, IV*b* and V*b* was found to be 0.56, 0.75 and 1.35 mmol g^{-1}, respectively. The CO_2 content of I*b*, III*b* and VI*b* was found to be negligibly small. I*a*–VI*a* showed no evolution of CO_2 when heated up to 1373 K. The values of basicity (STD and chemisorption of CO_2) for these catalysts are reported in this work after subtracting the values of their CO_2 content.

Fig. 3 shows the TPD curves of NH_3 from the catalysts, from their initial surface coverage by ammonia (θi) which corresponds to the total acidity.

It is seen that the acidity (measured in terms of NH_3 chemisorbed at 373 K) of La_2O_3 is strongly influenced by the precursor used in the catalyst preparation. The TPD curves (Fig. 3) show that the acid strength distribution on La_2O_3 is also very strongly influenced by the catalyst precursor. The presence of more than one peak in the TPD for all the catalysts reveals that there is more than one type of site for NH_3 chemisorption. The ammonia chemisorption site (*i.e.* acid site) on the catalyst is expected to be a surface La^{3+}. Thus, the results indicate that surface La^{3+} in different coordinations (3, 4 and 5 coordination) are present on the catalysts and their relative concentration is strongly influenced by the precursor.

It is interesting to note that I*a* has the highest acidity and contains only strong (major) and very strong (minor) acid sites compared with the other catalysts that are less acidic and also differ in their total acidity and acid strength distribution.

The temperature dependence of CO_2 chemisorption on the La_2O_3 catalysts calcined at 1023 and 1223 K is shown in Fig. 4. The chemisorption of CO_2 at higher temperature points to the involvement of stronger basic sites. Hence, the CO_2 chemisorption *vs.* temperature curves present the type of site energy distribution in which the number of sites are expressed in terms of the amount of CO_2 chemisorbed as a function of chemisorption temperature.

The results (Fig. 4) indicate that the basicity distribution on the catalysts is very broad and is strongly influenced by both the precursor and the calcination temperature. The observed base-strength distribution on the catalysts is expected to be due to the presence of surface O^{2-} sites (*i.e.* basic sites) in different coordinations (3, 4 and 5 coordination). The strong basicity is attributed to the low-coordinated O^{2-} surface sites.

The total concentration of basic sites (measured in terms of CO_2 chemisorbed at 323 K) is decreased on increasing the calcination temperature. This is expected to be mostly due to decrease in the surface area by catalyst sintering. Whereas, the larger decrease in the strong basic sites (measured in terms of CO_2 chemisorbed at 773 K), relative to that of the total basic sites, on increasing the calcination temperature (Table 2) is mostly due to the removal of crystal defects which results in a decrease in low-coordinated surface O^{2-}

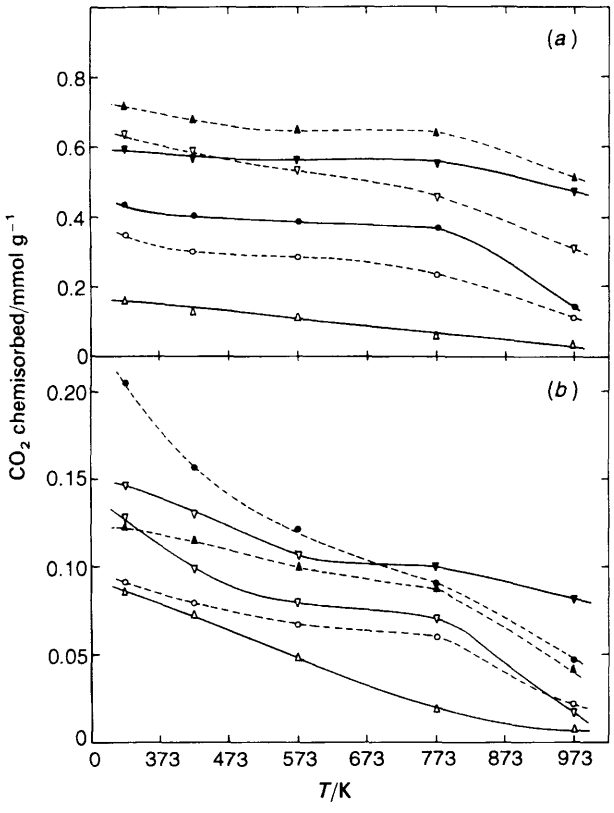

Fig. 4 Temperature dependence of chemisorption of CO_2 on (*a*) *b* catalysts and (*b*) *a* catalysts. ○, I; ●, II; △, III; ▼, IV; ▲, V and ▽, VI.

The observed changes in the surface acidity and basicity with changes in the preparation conditions are due to changes in the coordination number of surface La^{3+} and O^{2-} and probably also to the modification of the habits of the microcrystals produced with different crystal surface plane abundances.

Steady OCM

The OCM over I–VI*a* was carried out at 973–1123 K and with a CH_4/O_2 ratio of 4.0 and 8.0 at atmospheric pressure using very high space velocity (103 200 $cm^3\ g^{-1}\ h^{-1}$). The results showing the influence of temperature on the methane conversion, C_2 selectivity, C_2H_4/C_2H_6 and CO/CO_2 product ratios are presented in Fig. 5–7. The following general observations have been made:

(1) For all the catalysts the ethene/ethane ratio is increased with increasing temperature. This is consistent with earlier studies.[7,25,28–31]

(2) The temperature dependence of the CO/CO_2 ratio in the products is different for different catalysts. The CO/CO_2 ratio is decreased for II*a* and IV–VI*a* but passes through a minimum or maximum for I*a* and III*a*, depending upon the CH_4/O_2 ratio, with increasing temperature.

(3) For II*a* and IV–VI*a* the selectivity is increased with increasing temperature, the increase being very large for IV*a*. However, for I*a* and III*a* the selectivity is decreased for $CH_4/O_2 = 4.0$ but increased for $CH_4/O_2 = 8.0$ with increasing temperature.

(4) In general, the conversion is increased with increasing temperature. The increase is, however, very small for I–III*a* and V*a* at $CH_4/O_2 = 4.0$.

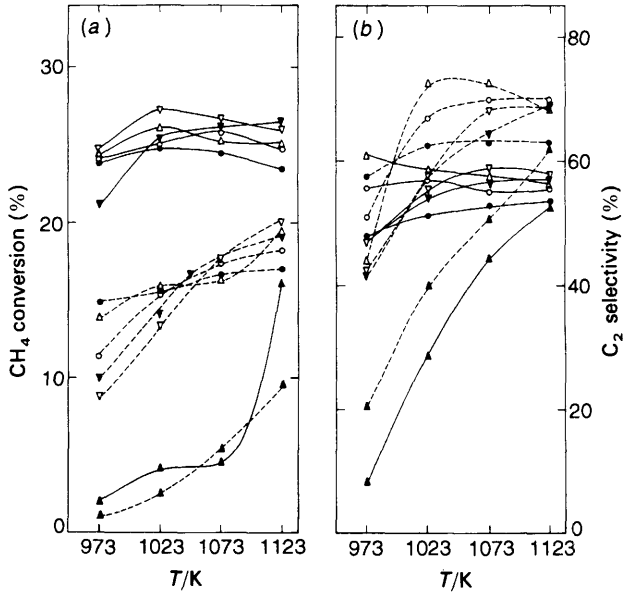

Fig. 5 Temperature dependence of (*a*) methane conversion and (*b*) C_2 selectivity of ○, I*a*; ●, II*a*; △, III*a*; ▲, IV*a*; ▽, V*a* and ▼, VI*a*

Table 2 Surface properties and catalytic activity and selectivity in OCM at 1023 and 1223 K, $CH_4/O_2 = 4.0$ and space velocity 103 200 $cm^3\ g^{-1}\ h^{-1}$

catalyst	surface area /$m^2\ g^{-1}$	acidity[a] /mmol g^{-1}	CO_2 content /mmol g^{-1}	basicity/mmol g^{-1} total[b]	basicity/mmol g^{-1} strong[c]	catalytic properties CH_4 conversion	C_2 selectivity	C_2 yield	C_2H_4/C_2H_6
calcined at 1023 K									
I	6.3	—	0.00	0.346	0.227	24.0	55.5	13.3	1.03
II	4.5	—	0.56	0.428	0.371	26.5	41.7	9.5	1.15
III	4.4	—	0.00	0.161	0.063	23.7	54.1	12.8	0.85
IV	3.0	—	0.75	0.602	0.567	22.2	55.2	12.3	1.60
V	2.1	—	1.35	0.710	0.640	23.7	51.4	12.2	1.00
VI	22.1	—	0.00	0.643	0.463	25.3	53.0	13.4	0.98
calcined at 1223 K									
I	3.8	1.69	0.00	0.091	0.056	25.0	57.0	14.3	1.11
II	6.3	0.69	0.00	0.205	0.040	24.8	51.5	12.8	0.90
III	1.7	0.24	0.00	0.091	0.019	26.2	56.8	14.9	0.85
IV	0.4	0.23	0.00	0.148	0.101	4.2	28.6	1.2	0.14
V	2.0	0.18	0.00	0.126	0.090	27.2	55.6	15.1	0.90
VI	2.7	0.17	0.00	0.126	0.074	25.6	54.7	14.0	0.86

[a] Measured in terms of NH_3 chemisorbed at 373 K. [b] Measured in terms of CO_2 chemisorbed at 323 K. [c] Measured in terms of CO_2 chemisorbed at 773 K.

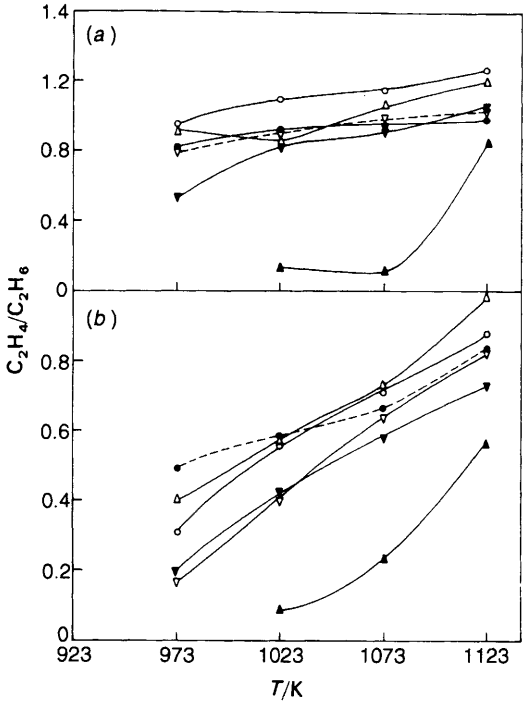

Fig. 6 Temperature dependence of ethene/ethane ratio over ○, I*a*; ●, II*a*; △, III*a*; ▲, IV*a*; ▽, V*a* and ▼, VI*a*. CH_4/O_2 : (*a*) 4 and (*b*) 8.

The above observations reveal a strong influence of catalyst precursor on the catalytic activity and selectivity in the OCM process.

The results (Fig. 5 and 6) also show that an increase in the CH_4/O_2 ratio from 4.0 to 8.0 causes a decrease in the conversion and the ethene/ethane ratio but the selectivity is generally increased. The influence of the CH_4/O_2 ratio is quite similar to that observed for OCM over rare-earth metal oxides,[7] MgO[29] and several other catalysts.[25,31]

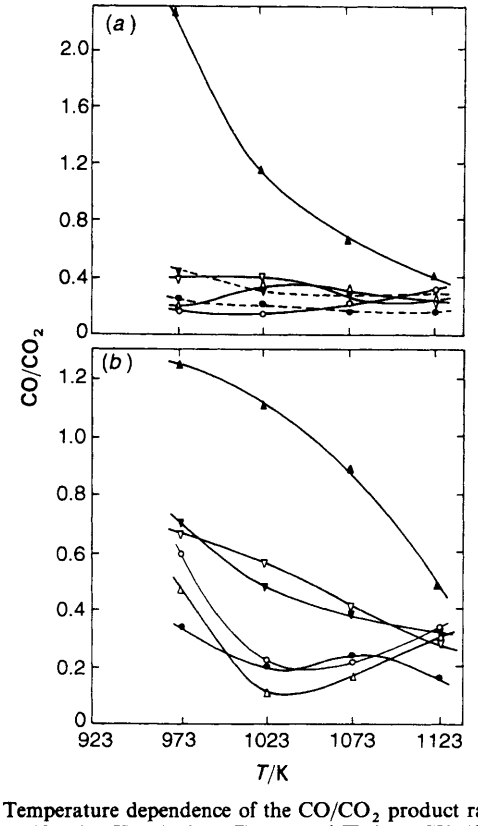

Fig. 7 Temperature dependence of the CO/CO_2 product ratio over ○, I*a*; ●, II*a*; △, III*a*; ▲, IV*a*; ▽, V*a* and ▼, VI*a*. CH_4/O_2: (*a*) 4 and (*b*) 8.

The results of OCM over I–VI*b* at 873–1023 K, CH_4/O_2 ratio of 4.0 and flow of 103 200 $cm^3\ g^{-1}\ h^{-1}$ (at 1 atm) are presented in Table 3. They show that, in OCM over catalysts calcined at 1023 K, the reaction temperature has a strong influence on the conversion and product selectivity. The methane conversion, C_2 selectivity and ethene/ethane ratio increase but the CO/CO_2 ratio decreases with increasing reaction temperature.

The increase in the ethene/ethane ratio with decreasing CH_4/O_2 ratio is most probably due to the availability of O_2 at higher concentration for the following gas-phase reactions involved in the formation of ethyl radicals and ethene from ethane.[32,33]

$$C_2H_6 + O_2 \rightarrow C_2H_5^{\bullet} + HO_2^{\bullet} \quad (1)$$

$$C_2H_5^{\bullet} + O_2 \rightarrow C_2H_4 + HO_2^{\bullet} \quad (2)$$

$$C_2H_6 + HO_2^{\bullet} \rightarrow C_2H_5^{\bullet} + H_2O_2 \quad (3)$$

$$H_2O_2 + Z \rightarrow 2OH^{\bullet} + Z \quad (4)$$

(where Z is a third body, *e.g.* water molecule)

$$C_2H_6 + OH^{\bullet} \rightarrow C_2H_5^{\bullet} + H_2O \quad (5)$$

Ethane is expected to be formed by gas-phase coupling of methyl radicals.[34]

The increase in the ethene/ethane ratio with increasing temperature is expected to be due to the decomposition of ethyl radicals formed in reactions (1), (3) and (5) and thermal cracking of ethane at the higher temperatures

$$C_2H_5^{\bullet} \rightarrow C_2H_4 + H^{\bullet} \quad (6)$$

$$C_2H_6 \rightarrow C_2H_4 + H_2 \quad (7)$$

It may also be due to the increase in the rate of the gas-phase reaction of ethyl radicals to form ethene [reaction (2)] and the oxidative dehydrogenation of ethane on the catalyst surface.

The increase in the C_2 selectivity with increasing temperature is expected to be mostly due to a decrease in the formation of carbon oxides from methyl radicals by the following gas-phase reaction.[34]

$$CH_3^{\bullet} + O_2 \rightarrow CH_3O_2^{\bullet} \rightarrow \rightarrow CO, CO_2 \quad (8)$$

The formation of methylperoxy radicals ($CH_3O_2^{\bullet}$), which leads to CO and CO_2, is not favoured at higher temperatures[2,34] and hence the C_2 selectivity is expected to increase with the temperature. However, the decrease in the selectivity at the higher temperatures in some cases (Fig. 5) is attributed mostly to the conversion of methyl radicals to CO and CO_2 on the catalyst surface. To a small extent, it may also be due to combustion of ethane and ethene in the gas phase and/or on the catalyst surface at the higher temperatures.

Note that unsteady reaction behaviour showing oscillations has been observed for II*b* in a narrow temperature range $853 < T/K < 933$. However, no unsteady (*i.e.* oscillating) reaction over the other catalysts at 933–1023 K was observed.

The unsteady/steady OCM over La_2O_3 II*a*, II*b* and II*c* catalysts at different reaction conditions is discussed later.

Comparison of Catalyst Surface Properties, Activity and Selectivity in Steady OCM

The catalysts (I–VI), calcined at 1023 and 1223 K are compared for their surface properties and catalytic activity and selectivity in the steady OCM at 1023 K in Table 2.

Table 3 OCM over La_2O_3 catalyst calcined at 1023 K

catalyst	reaction temperature/K	CH_4 conversion (%)	C_2 selectivity (%)	C_2H_4/C_2H_6	CO/CO_2
I*b*	873	15.7	29.7	0.37	0.56
	923	21.5	47.0	0.71	0.39
	973	23.5	53.6	0.92	0.33
	1023	24.0	55.5	1.03	0.25
II*b*	873	23.1	49.3	0.83	0.29
	883–923	oscillations observed			
	973	24.9	46.3	0.89	0.31
	1023	26.5	47.6	0.98	0.28
III*b*	873	11.2	36.5	0.56	0.56
	923	14.7	38.3	0.56	0.54
	973	18.9	46.3	0.66	0.45
	1023	23.7	54.1	0.85	0.39
IV*b*	873	12.7	53.6	0.86	0.50
	923	20.8	55.2	0.97	0.43
	973	22.0	54.9	1.21	0.37
	1023	22.2	55.2	1.60	0.33
V*b*	873	6.9	10.0	<0.1	0.74
	923	22.7	42.7	0.63	0.45
	973	22.2	48.5	0.71	0.40
	1023	23.7	51.4	1.00	0.39
VI_b	873	17.0	38.9	0.70	0.47
	923	19.8	39.8	0.72	0.37
	973	22.3	46.2	0.73	0.36
	1023	25.3	53.0	0.98	0.29

Reaction conditions: amount of catalyst = 0.1 g, CH_4/O_2 ratio = 4.0 and space velocity (at STP) = 103 200 $cm^3\ g^{-1}\ h^{-1}$.

The very low surface area and catalytic activity and selectivity of IV*a* (Table 2) may be due to sintering of the catalyst, probably related to the presence of traces of sodium in the La carbonate (I) obtained by precipitation with sodium carbonate.

The increase in the catalyst calcination temperature from 1023 to 1223 K resulted in a large decrease in the surface area and basicity (both total and strong basicity) but, except for IV, a significant increase in both the methane conversion activity and selectivity, and also caused a change in the catalyst order for their surface and catalytic properties.

The above comparison and the results in Fig. 1–7 and Tables 1–3 reveal a strong influence of the catalyst preparation conditions on the surface properties and catalytic activity and selectivity, in steady OCM. From the comparison of the catalysts for their surface acidity and/or basicity with that for the catalytic activity, C_2 selectivity or C_2 yield, it can be noted that there is no direct relationship between the surface acidity/basicity and the catalytic activity or selectivity, as observed for rare-earth oxides.[7] Also, in our earlier studies on the OCM over alkali- or rare-earth-metal promoted MgO and CaO[25,31] and alkali- or alkaline-earth-metal promoted rare-earth metal oxides,[25] no direct relationship between the surface and catalytic properties was observed. The overall OCM process is very complex. It involves a number of catalytic (*i.e.* surface-catalysed) and non-catalytic (homogeneous or surface-initiated homogeneous) reactions occurring simultaneously.[34–36] The contribution of the homogeneous reactions to the observed conversion and selectivity in the OCM process is quite appreciable and hence it is difficult to obtain a direct relationship between the surface properties and the catalytic activity and selectivity.

Unsteady Reaction Behaviour

The results indicate that only II, prepared from La acetate, shows unsteady reaction behaviour in OCM over a narrow temperature range. In the earlier studies[1–7,37–39] oscillations were not observed.

In our earlier paper,[23] the results showing periodic fluctuations in reaction temperature and O_2 concentration (in the product) indicate symmetric oscillations in OCM over II*b* above 823 K but below 973 K. Additional results showing the influence of process parameters and catalyst parameters on the oscillatory behaviour in the OCM process over II are presented in Tables 4–6. The minimum and maximum of the O_2 concentration oscillation correspond to the maximum and minimum, respectively, of the temperature oscillation. Note that the results of OCM under the unsteady conditions are indicative of changes in the conversion and product selectivity measured at close to the minimum and maximum of the oscillating reaction temperatures. It is extremely difficult to obtain results exactly at the minimum and maximum of the oscillating temperature.

Effect of Process Parameters

The influence of CH_4/O_2 ratio (in the feed) on the steady/unsteady reaction behaviour for the OCM process over II is shown in Table 4. The temperature and O_2 concentration oscillations are observed only over a narrow temperature range, depending upon the CH_4/O_2 ratio. For ratios 3.0, 4.0 and 5.0, the oscillations are observed only at $843 < T/K < 943$, $863 < T/K < 933$ K and $873 < T/K < 903$, respectively; for $CH_4/O_2 \geqslant 6.0$, no oscillations were observed. Both the observed temperature and O_2 concentration oscillations were symmetrical and sustained for a long period without affecting their amplitude [*i.e.* $T_{max} - T_{min}$ and $C_{O_2(max)} - C_{O_2(min)}$] and cycle period. The recorded oscillations were given elsewhere.[23,25] In general, the cycle period and amplitude of both the oscillations are found to decrease with increasing reactor temperature.

A comparison of the results in Table 5 with that in Table 4 for a CH_4/O_2 ratio of 4.0 show a high dependence on the amount of catalyst on the reaction behaviour. When the amount of catalyst in the reactor is changed from 0.1 g (Table 4) to 0.2 g (Table 5), then, at the same space velocity (103 200 $cm^3\ g^{-1}\ h^{-1}$) oscillations are observed at 883, 903 and 923 K only for the smaller amount of catalyst. This indicates that when the linear or superficial gas velocity is doubled, the

Table 4 OCM over II under steady and unsteady conditions at different CH_4/O_2 ratios

CH_4/O_2	reactor temperature/K	oscillating temperature/K	oscillating O_2 concentration in product (mol%)	methane conversion (%)	C_2 selectivity	C_2H_4/C_2H_6	CO/CO_2
			II*b*				
3.0	853	800 ± 5 (min)	18.0 ± 0.5 (max)	16.3	27.2	0.95	0.32
		1005 ± 6 (max)	5.5 ± 0.4 (min)	28.6	43.0	1.06	0.10
	873	838 ± 3 (min)	15.3 ± 0.2 (max)	18.9	29.1	0.83	0.72
		1003 ± 2 (max)	5.6 ± 0.2 (min)	22.4	42.6	1.01	0.20
	923	924 ± 2 (min)	8.7 ± 0.2 (max)	22.4	33.1	0.76	0.25
		964 ± 5 (max)	7.2 ± 0.2 (min)	23.4	37.6	0.86	0.33
	973[a]	973 ± 5	6.2 ± 0.1	24.4	40.9	0.86	0.23
	1023[a]	1023 ± 2	4.7 ± 0.1	28.6	44.0	1.20	0.15
4.0	883	885 ± 2 (min)	10.2 ± 0.1 (max)	23.2	48.8	0.88	0.20
		989 ± 6 (max)	5.2 ± 0.3 (min)	24.0	48.3	0.85	0.25
	903	913 ± 2 (min)	8.8 ± 0.2 (max)	22.5	47.0	0.82	0.23
		975 ± 4 (max)	6.0 ± 0.2 (min)	22.0	43.8	0.83	0.30
	923	933 ± 3 (min)	7.7 ± 0.1 (max)	20.8	42.2	0.80	0.35
		971 ± 6 (max)	6.2 ± 0.1 (min)	22.2	44.9	0.82	0.26
	973[a]	973 ± 2	6.0 ± 0.2	24.9	46.3	0.89	0.31
	1023[a]	1023 ± 3	4.9 ± 0.1	26.5	47.6	0.98	0.28
5.0	883	868 ± 2 (min)	13.1 ± 0.2 (max)	5.9	16.0	0.21	0.70
		931 ± 5 (max)	9.7 ± 0.3 (min)	7.7	30.0	0.27	0.28
	923[a]	923 ± 5	9.2 ± 0.2	10.0	30.4	0.31	0.50
	973[a]	973 ± 3	6.5 ± 0.1	12.0	30.8	0.35	0.77
	1023[a]	1023 ± 2	4.9 ± 0.3	19.1	50.4	0.69	0.26
6.0	883[a]	883 ± 2	11.5 ± 0.1	3.7	5.7	—	0.91
	923[a]	923 ± 3	8.5 ± 0.1	8.5	25.8	0.21	0.59
	973[a]	973 ± 5	6.0 ± 0.2	14.4	42.8	0.43	0.41
	1023[a]	1023 ± 2	4.9 ± 0.1	16.8	51.3	0.60	0.28
			II*c*				
4.0	873[a]	873 ± 2	2.6 ± 0.1	23.1	49.3	0.83	0.29
	923[a]	923 ± 3	2.2 ± 0.1	23.7	48.9	0.94	0.29
	973[a]	973 ± 1	1.9 ± 0.3	23.5	46.9	1.02	0.33
	1023[a]	1023 ± 1	1.8 ± 0.1	22.9	41.7	1.15	0.39
			II*a*				
4.0	873[a]	873 ± 2		No reaction			
	923[a]	889 ± 2 (min)	—	5.2	14.1	0.15	0.50
		996 ± 3 (max)	—	18.2	46.7	0.74	0.27
	973[a]	973 ± 3	—	23.9	48.0	0.82	0.23
	1073[a]	1073 ± 4	—	24.5	53.3	0.96	0.17

Reaction conditions; amount of catalyst, 0.1 g; feed, CH_4–O_2 mixture of pure CH_4 and O_2 and space velocity 103 200 $cm^3\ g^{-1}\ h^{-1}$. [a] Oscillations not observed.

Table 5 OCM over II*b* under steady and unsteady conditions at different space velocities

run no.	reactor temperature/K	oscillating temperature/K	oscillating O_2 concentration in products (mol%)	methane conversion (%)	C_2 selectivity (%)	C_2H_4/C_2H_6	CO/CO_2
			space velocity 51 600 $cm^3\ g^{-1}\ h^{-1}$				
1	823	823 ± 2		no reaction			
2	883[a]	883 ± 2	3.5 ± 0.1	26.4	46.7	0.82	0.22
3	903[a]	903 ± 5	3.0 ± 0.2	28.8	46.9	0.87	0.27
4	923[a]	923 ± 3	2.8 ± 0.3	27.4	49.9	0.91	0.16
5	973[a]	973 ± 3	2.5 ± 0.1	28.6	49.0	0.99	0.26
6	1023[a]	1023 ± 5	2.9 ± 0.1	28.2	50.7	1.05	0.17
7	823	782 ± 1 (min)	9.2 ± 0.2 (max)	18.5	42.5	0.82	0.40
		925 ± 5 (max)	3.0 ± 0.1 (min)	27.6	41.3	0.89	0.44
8	773	773 ± 1	20.0 ± 0.1	no reaction			
			space velocity 103 200 $cm^3\ g^{-1}\ h^{-1}$				
1	823	823 ± 2		no reaction			
2	873[a]	873 ± 5	7.5 ± 0.2	19.6	46.1	0.96	0.40
3	923[a]	923 ± 3	4.0 ± 0.1	24.0	43.1	1.21	0.54
4	973[a]	973 ± 3	3.5 ± 0.3	23.7	41.3	1.35	0.55
5	1023[a]	1023 ± 2	3.0 ± 0.2	23.2	40.2	1.52	0.55
6	833[a]	833 ± 3	12.5 ± 0.3	11.1	47.8	0.78	0.21
7	808	784 ± 3 (min)	16.0 ± 0.2 (max)	5.8	32.8	0.56	0.49
		878 ± 5 (max)	11.5 ± 0.1 (min)	13.3	45.3	0.62	0.42
8	773	773 ± 1	20.0 ± 0.1	no reaction			

Reaction conditions: amount of catalyst, 0.2 g and CH_4/O_2 ratio in feed, 4.0. [a] Oscillations not observed.

Table 6 OCM over II*b* with particle size of 30–72 mesh, under steady and unsteady conditions

run no.	reactor temperature/K	oscillating temperature/K	oscillating O_2 concentration in products (mol%)	methane conversion (%)	C_2 selectivity (%)	C_2H_4/C_2H_6	CO/CO_2
1	823	823 ± 2		no reaction			
2	873[a]	873 ± 2	3.8 ± 0.2	26.0	44.9	1.01	0.28
3	923[a]	923 ± 5	3.5 ± 0.1	26.7	45.8	1.08	0.27
4	973[a]	973 ± 3	3.2 ± 0.2	28.1	47.0	1.05	0.27
5	1023[a]	1023 ± 5	3.1 ± 0.1	28.3	47.7	1.18	0.26
6	833[a]	833 ± 2	6.8 ± 0.2	23.8	45.3	0.93	0.30
7	773[a]	773 ± 5	9.0 ± 0.1	20.8	42.5	0.85	0.36
8	723	715 ± 8 (min)	16.7 ± 0.1 (max)	13.3	40.1	0.77	0.36
		765 ± 6 (max)	12.5 ± 0.2 (min)	15.1	40.7	0.78	0.39
9	673	673 ± 1	20.0 ± 1	no reaction			

Reaction conditions: amount of catalyst, 0.1 g, CH_4/O_2 ratio in feed, 4.0 and space velocity 103 200 $cm^3\ g^{-1}\ h^{-1}$. [a] Oscillations not observed.

unsteady reaction behaviour changes drastically. It is also interesting to note from the results in Table 5 that, for both space velocities the catalyst do not show any activity initially at or below 823 K but after the reaction at higher temperatures, it shows activity with oscillations at 823 K for a space velocity 51 600 $cm^3\ g^{-1}\ h^{-1}$ and at 808 K for velocity 103 200 $cm^3\ g^{-1}\ h^{-1}$. These observations indicates a possibility of formation of active sites responsible for the unsteady behaviour during the reaction at the higher temperatures. The increase in the space velocity resulted in a decrease in the temperature at which the oscillations occurred and also a decrease in the amplitude of both the oscillations.

Effect of Catalyst Parameters

A comparison of the results on II*a*, II*b* and II*c* for $CH_4/O_2 = 4.0$ (Table 4) shows that the catalyst calcination conditions (temperature and gas atmosphere, *i.e.* N_2 or O_2) have a strong influence on the unsteady reaction behaviour and also on the catalytic properties in steady OCM.

In the OCM over II*c*, no oscillations were observed and the C_2 selectivity was found to decrease with increasing reaction temperature. With II*a* and II*b*, oscillations are observed and the C_2 selectivity is found to increase with increasing reaction temperature. These observations reveal a strong influence of the gas atmosphere used in the catalyst calcination on the reaction behaviour and selectivity in the OCM process.

The results on II*a* and II*b* (for $CH_4/O_2 = 4.0$) indicate that, when the catalyst calcination temperature is increased from 1023 to 1223 K, no reaction occurs at 873 K and the oscillations are observed only at 923 K, thus narrowing drastically the temperature range for the unsteady reaction.

A comparison of the results in Tables 4 and 6 shows that for II*b* (at $CH_4/O_2 = 4.0$) when the particle size of the catalyst is changed from 22–30 mesh to 30–72 mesh, no unsteady reaction behaviour in the OCM was observed at 873–923 K but it was observed at 723 K after the reaction at higher temperatures. The results in Table 6 also reveal that, in this case, no catalytic activity was observed at 823 K but the catalyst showed activity at lower temperature after the reaction at higher temperatures, indicating the creation of new catalytic active sites on the catalyst during the OCM reaction at the higher temperatures.

The above observations reveal that the unsteady reaction behaviour in the OCM process over II is very complex and strongly influenced by both the process and catalyst parameters. Also, new sites, active at lower temperatures, are formed on the catalyst during the OCM at higher temperatures. However, the nature of these sites has not been identified; further work is necessary for this.

The observed unsteady reaction behaviour is likely to be due to a large difference in the C_2 selectivity of the La_2O_3 catalyst in the OCM process at lower (<973 K) and higher (>973 K) temperatures (Table 4); the selectivity is decreased with decreasing temperature. In the pulse reaction of methane over II*a* in presence of free O_2 ($CH_4/O_2 = 2.9$), the C_2 selectivity at lower temperatures (823–923 K) was found to be much smaller (almost negligibly small) than at higher temperatures (⩾973 K).[25] With II*c*, the selectivity decreases with increasing temperature (Table 4) and, therefore, no oscillations are observed. In addition to the above the unsteady-state reaction behaviour could also be due to a change in the nature of the active sites on the catalyst. There is a possibility of the formation of surface La oxycarbonate (which is stable at lower temperatures) during the reaction at higher temperatures. Since, the unsteady reaction behaviour is observed only in the case of a particular catalyst sample, the temperature controller is not expected to have a significant role in the observed oscillations.

Conclusions

The following important conclusions have been drawn from the present investigation on the surface properties, the catalytic activity and selectivity, and the steady or unsteady reaction behaviour in OCM of La_2O_3 catalysts prepared using different catalyst precursors and calcination conditions:

(1) The surface properties (*viz.* surface area, crystal size and morphology, acidity and acid-strength distribution, basicity and base-strength distribution) and the catalytic activity and selectivity in OCM are strongly influenced by the catalyst precursor [*viz.* hydrated La_2O_3, La nitrate, La acetate, La carbonate and La hydroxide]. The calcination temperature also has a strong influence on the surface and catalytic properties of La_2O_3 obtained from the different precursors. There is no direct relationship between the surface acidity/basicity of La_2O_3 and its catalytic activity and selectivity in OCM.

(2) Among the La_2O_3 catalysts, only the one obtained from La acetate and calcined in the presence of N_2 (but not in O_2) shows unsteady reaction behaviour with symmetrical temperature and concentration oscillations in the OCM process at below 933 K in a narrow temperature range.

(3) The unsteady reaction behaviour in OCM on the La_2O_3 catalyst obtained from La acetate is very complex and strongly influenced by both the process parameters (*viz.* temperature, CH_4/O_2 ratio in feed, space velocity and linear or superficial gas velocity) and catalyst parameters (*viz.* particle size and calcination temperature and gas atmosphere used in the catalyst calcination). There is a strong possibility of for-

mation on the catalyst of new sites catalytically active at lower temperatures (below 873 K) during the OCM at higher temperatures.

The authors are grateful to Dr. Kuber and Dr. Belhekar (National Chemical Laboratory, Pune) for their help in the catalyst characterization by XRD and SEM.

References

1 K. Otsuka, K. Jinno and A. Morikawa, *Chem. Lett.*, 1985, 499.
2 C. H. Lin, K. D. Campbell, J. X. Wang and J. H. Lunsford, *J. Phys. Chem.*, 1986, **90**, 534.
3 K. Otsuka, K. Jinno and A. Morikawa, *J. Catal.*, 1986, **100**, 353.
4 K. D. Campbell, H. Zhang and J. H. Lunsford, *J. Phys. Chem.*, 1988, **92**, 750.
5 S. J. Korf, J. A. Roos, H. M. Diphoorn, R. H. J. Veehof, J. G. van Ommen and J. R. H. Ross, *Catal. Today*, 1989, **4**, 279.
6 R. P. Taylor and G. L. Schrader, *Ind. Eng. Chem. Res.*, 1991, **30**, 1016.
7 V. R. Choudhary and V. H. Rane, *J. Catal.*, 1991, **130**, 411.
8 A. Kooh, H. Mimoun and C. J. Cameron, *Catal. Today*, 1989, **4**, 333.
9 R. Burch, G. D. Squire and S. C. Tsang, *Appl. Catal.*, 1988, **43**, 105.
10 Y. Tong, M. P. Rosynek and J. H. Lunsford, *J. Catal.*, 1990, **126**, 291.
11 J. M. Deboy and R. B. Hicks, *J. Chem. Soc., Chem. Commun.*, 1988, 982.
12 J. M. Deboy and R. B. Hicks, *J. Catal.*, 1988, **113**, 517.
13 Y. Feng, J. Niiranen and D. Gutman, *J. Phys. Chem.*, 1991, **95**, 6558; 6564.
14 J. M. Deboy and R. B. Hicks, *Ind. Eng. Chem. Res.*, 1988, **27**, 1577.
15 E. E. Gulcicek, S. D. Colson and L. D. Pfefferle, *J. Phys. Chem.*, 1990, **94**, 7069.
16 M. Xu and J. H. Lunsford, *Catal. Lett.*, 1991, **11**, 295.
17 Z. Kalenik and E. E. Wolf, *Catal. Today*, 1992, **13**, 255.
18 H. Yamashita, Y. Machida and A. Tomita, *Appl. Catal.*, 1991, **79**, 203.
19 V. R. Choudhary, S. T. Chaudhari, A. M. Rajput and V. H. Rane, *J. Chem. Soc., Chem. Commun.*, 1989, **555**, 1526.
20 V. R. Choudhary, S. T. Chaudhari, A. M. Rajput and V. H. Rane, J. Chem. Soc., Chem. Commun., 1989, 605.
21 V. R. Choudhary, S. T. Chaudhari, A. M. Rajput and V. H. Rane, *Catal. Lett.*, 1989, **3**, 85.
22 S. Becker and M. Baerns, *J. Catal.*, 1991, **128**, 512.
23 V. R. Choudhary and V. H. Rane, *Catal. Lett.*, 1992, **16**, 211.
24 V. R. Choudhary and V. H. Rane, *Catal. Lett.*, 1990, **4**, 101.
25 V. H. Rane, Ph.D. Thesis, University of Pune, 1992.
26 S. Bernal, R. Garcia, J. M. Lopez and J. M. Rodriguez-Jzquierdo, *Collect. Czech. Chem. Commun.*, 1983, **48**, 2205.
27 I. Carrizosa, J. A. Odriozola and J. M. Trillo, *Inorg. Chim. Acta*, 1984, **94**, 114.
28 J. B. Kimble and J. H. Kolts, *CHEMTECH.*, 1987, 501.
29 V. R. Choudhary and V. H. Rane, *J. Catal.*, 1994, **145**, 300.
30 V. R. Choudhary, A. M. Rajput, D. B. Akolekar and V. A. Seleznev, *Appl. Catal.*, 1990, **62**, 171.
31 S. T. Chaudhari, Ph.D. Thesis, University of Bombay, 1993.
32 E. Morales and J. H. Lunsford, *J. Catal.*, 1989, **118**, 255.
33 R. A. Geisbrecht and T. E. Daubart, *Ind. Eng. Chem. Process Des. Dev.*, 1975, **14**, 159.
34 T. Ito, J. X. Wang, C. H. Lin and J. H. Lunsford, *J. Am. Chem. Soc.*, 1985, **107**, 5062.
35 V. R. Choudhary, S. T. Chaudhari and A. M. Rajput, *AIChE J.*, 1991, **37**, 915.
36 V. R. Choudhary and V. H. Rane, *J. Catal.*, 1992, **135**, 310.
37 S. Lacombe, J. G. Sanchez, M. P. Delichere, H. Mozzanego, J. M. Tatiouet and C. Mirodatos, *Catal. Today*, 1992, **13**, 273.
38 C. Louis, T. L. Chang, M. Kermarec, T. L. Van, J. M. Tatiouet and M. Che, *Catal. Today.*, 1992, **13**, 283.
39 T. L. Van, C. Louis, M. Kermarec and J. M. Tatiouet, *Catal. Today*, 1992, **13**, 321.

Paper 4/01718H; *Received* 22*nd March*, 1994